DOI: https://doi.org/10.15407/pmach2020.02.021

UDC 53:002

NON-STATIONARY RESPONSE OF A CARBON NANOTUBE-REINFORCED COMPOSITE CONICAL SHELL

Kostiantyn V. Avramov
kvavramov@gmail.com
ORCID: 0000-0002-8740-693X

Borys V. Uspenskyi
Uspensky.kubes@gmail.com
ORCID: 0000-0001-6360-7430

Nataliia H. Sakhno
natali.sahno@gmail.com
ORCID: 0000-0003-4179-5316

Iryna V. Biblik
i.v.biblik@gmail.com
ORCID: 0000-0002-8650-1134

A. Podgorny Institute of Mechanical Engineering Problems of NASU
2/10, Pozharskyi St., Kharkiv, 61046, Ukraine

This paper is devoted to the development of a method for the analysis of the non-stationary deformation of a carbon nanotube-reinforced composite shell under pulsed loading. The development of innovative manufacturing technologies has led to the emergence of new materials that have high potential for use in the aerospace industry. In particular, these include carbon nanotube-reinforced materials, or so-called nanocomposites. These materials demonstrate high strength and rigidity in combination with low weight, which is especially important when designing components of rocket and aircraft structures: fairings, fuel tanks, engines. At the same time, the behavior of structural elements under typical environmental influences requires additional studies due to the anisotropic and functional-gradient properties of materials. The determination of the mechanical properties of a nanocomposite is a known difficulty due to its anisotropic nature. There are various approaches to solving this problem. The simplest and at the same time well-proven one is the modified mixing rule, which is used in the paper. Equations of motion of the conical shell under the action of shock loading are obtained. To derive the equations of motion of the shell, a high-order theory is used that takes into account shifts and rotational inertia. To analyze the non-stationary dynamics of the shell, its free vibrations are analyzed. The analysis results are highly accurate compared to the finite element calculation carried out in the ANSYS software suite. A method is proposed for analyzing the dynamical response of the shell under the action of impact loading, which is based on the eigenvibration analysis of structures. Time dependencies of adapter deformations are obtained for the cases of actuation of two and four symmetrically arranged pyrodevices. The results of the analysis of the non-stationary dynamics of the adapter were compared with the finite element analysis results.

Keywords: *conical shell, pulsed load, non-stationary process, nanocomposite material.*

Introduction

In recent decades, nanotechnology is increasingly penetrating the practice of designing and manufacturing engineering structures and processes. With the help of nanotechnology, new materials are created, which include nanocomposites. The reinforcing elements of nanocomposites are carbon nanotubes, which have Young's modulus and tensile strength several orders of magnitude higher than that of steel. The use of these materials is especially relevant in the design of rocket and airframe structure components: fairings, fuel tanks, power plants.

A number of studies have been carried out to determine the mechanical characteristics of nanocomposites. In [1], micromechanics methods are used to numerically simulate the effective elastic properties of nanocomposites. In [2], these properties are determined by the finite element approach based on the continuum mechanical model. In [3], a model is proposed by which the properties of nanocomposites are determined taking into account the interactions between atoms in a molecular model.

Experimental studies of the mechanical properties of nanocomposites are reflected in [4–7]. In [4], in the course of compression experiments, it is shown that the yield strength of a rubber specimen increases significantly – by a factor of two at a carbon nanotube volume fraction of 1% and four times, at that of 4%. In [5], it is found that the Young's modulus of oriented nanocomposites can be five times higher than that of the nanocomposites in which carbon nanotubes are randomly oriented. The authors calculate the Young's modulus of a nanocomposite with a small error, using the modified mixing rule. In [6], a mixing rule is proposed, differing significantly from that used in other similar works. The review article [7] presents various micromechanical models for assessing the mechanical properties of nanocomposites.

In a number of works, the statics and dynamics of carbon nanotube-reinforced composite shells are studied based on their linear models. The statics and dynamics of cylindrical carbon nanotube-reinforced composite shells are considered in [8–12]. Linear vibrations of carbon nanotube-reinforced composite plates are studied in [13–15]. Free vibrations of functionally gradient double-curvature flat shells reinforced with graphene nanoplates are studied in [16, 17]. A dynamic analysis of cylindrical composite shells reinforced with single-walled carbon nanotubes under the action of shock loading is described in [18].

This paper describes a method for analyzing vibrations of a nanocomposite shell under the action of shock loading. This process corresponds to the behavior of the rocket body after the adapter is jettisoned with the help of pyrodevices.

Mechanical Properties of Nanocomposites

To determine the mechanical properties of nanocomposites, the mixing rule is used, which has proven itself well in evaluating the properties of nanocomposites. We consider the nano-reinforced material in which carbon nanotubes are placed along the shell generatrix. The main types of reinforcement (Fig. 1) suggest a linear change in the thickness of the volume density of carbon nanotubes in the material. So, with a UD reinforcement, the volume density of carbon nanotubes in the material is constant; with a V reinforcement, it is insignificant on the inner surface of the shell, and reaches its maximum on the outer one; with an X reinforcement, an equal maximum density of carbon nanotubes is achieved on the outer and inner surfaces of the shell, and on the middle one it is zero.

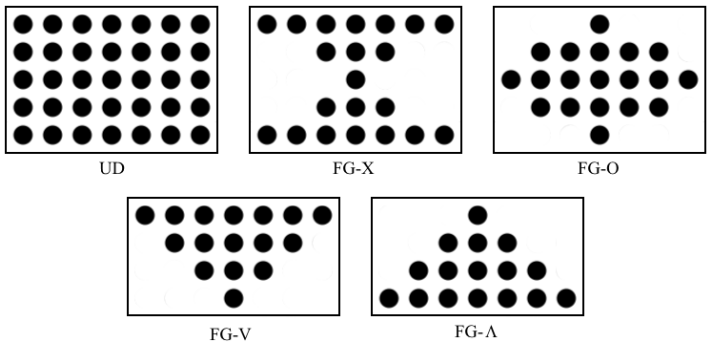

Fig. 1. Types of shell reinforcement with carbon nanotubes in the transverse direction

Denote by V_{CNT}^{*} the part of volume occupied by uniformly distributed carbon nanotubes. Then, for each type of reinforcement, the part of volume occupied by carbon nanotubes, $V_{CNT}(z)$, is described by the following formulas [16, 19, 20]:

– for UD-CNT $V_{CNT}(z) \equiv V_{CNT}^{*}$;

– for FGV-CNT $V_{CNT}(z) = \left(1 + \frac{2z}{h}\right) V_{CNT}^{*}$;

– for FGΛ-CNT $V_{CNT}(z) = \left(1 - \frac{2z}{h}\right) V_{CNT}^{*}$;

– for FGX-CNT $V_{CNT}(z) = \frac{4|z|}{h} V_{CNT}^{*}$;

– for FGO-CNT $V_{CNT}(z) = 2\left(1 - \frac{2|z|}{h}\right) V_{CNT}^{*}$.

The mechanical characteristics of the functionally gradient composite material of the cylindrical shell depend on the transverse coordinate z. They are estimated using the mixing rule as follows [19, 20]:

$$E_{11}(z) = \eta_1 V_{CNT}(z) E_{11}^{CNT} + V_m(z) E^m, \quad E_{22}(z) = \frac{\eta_2 E_{22}^{CNT} E^m}{V_{CNT}(z) E^m + V_m(z) E_{22}^{CNT}}, \quad G_{12}(z) = \frac{\eta_3 G_{12}^{CNT} G^m}{V_{CNT}(z) G^m + V_m(z) G_{12}^{CNT}},$$

$$\mu_{12}(z) = V_{CNT}(z) \mu_{12}^{CNT} + V_m(z) \mu^m, \quad \mu_{21}(z) = \frac{\mu_{12}(z)}{E_{11}(z)} E_{22}(z),$$

$$\rho(z) = V_{CNT}(z) \rho^{CNT} + V_m(z) \rho^m, \quad V_m(z) = 1 - V_{CNT}(z),$$

where $E_{11}^{CNT}, E_{22}^{CNT}, G_{12}^{CNT}$ are Young's moduli and the shear modulus of carbon nanotubes; μ_{12}^{CNT} is the Poisson's ratio of carbon nanotubes; η_1, η_2, η_3 are reinforcement efficiency parameters; E^m, G^m are Young's and shear moduli; ρ^{CNT}, ρ^m are the carbon nanotube and matrix densities.

Since the shell material is functionally-gradient, shear will be taken into account in the design model [21, 22]. In addition to the elastic constants presented above, it is necessary to determine the shear moduli. Following article [16], they are defined as follows: $G_{13}(z) = G_{12}(z); G_{23}(z) = G_{12}(z)$.

Hooke's law for the composite material of the shell has the form

$$\begin{bmatrix} \sigma_{xx} \\ \sigma_{\theta\theta} \end{bmatrix} = \begin{bmatrix} Q_{11}(z) & Q_{12}(z) \\ Q_{21}(z) & Q_{22}(z) \end{bmatrix} \begin{bmatrix} \varepsilon_{xx} \\ \varepsilon_{\theta\theta} \end{bmatrix}, \quad \sigma_{\theta z} = G_{23}(z)\gamma_{\theta z}, \quad \sigma_{xz} = G_{13}(z)\gamma_{xz}, \quad \sigma_{x\theta} = G_{12}(z)\gamma_{x\theta},$$

$$Q_{11}(z) = \frac{E_{11}(z)}{1-\mu_{12}(z)\mu_{21}(z)}, \quad Q_{22}(z) = \frac{E_{22}(z)}{1-\mu_{12}(z)\mu_{21}(z)}, \quad Q_{12}(z) = \frac{\mu_{21}(z)E_{11}(z)}{1-\mu_{12}(z)\mu_{21}(z)},$$

where $\gamma_{xz}, \gamma_{\theta z}$ are shear strains; $\varepsilon_{xx}, \varepsilon_{\theta\theta}, \gamma_{\theta z}, \gamma_{xz}, \gamma_{x\theta}$ are elements of the strain tensor; $\sigma_{xz}, \sigma_{\theta z}$ are shear stresses; $\sigma_{xx}, \sigma_{\theta\theta}, \sigma_{x\theta}$ are elements of the stress tensor.

Basic Equations of the Non-stationary Conical Shell Response

The non-stationary dynamics of the conical shell will be studied in a curvilinear coordinate system (Fig. 2).

The *x* axis is directed along the generatrix of the median surface of the conical shell. The φ axis describes the circumferential coordinate of the conical shell. The circles of the median surface, whose planes are parallel to the base, have a radius *r*: $r = x \cdot \sin\alpha$. We denote the radius of curvature of this cone surface along the circumference by $R_\varphi = x \cdot \mathrm{tg}(\alpha)$. The *z* axis is perpendicular to the median surface and directed outward of the structure.

Since the conical shell under consideration is a nanocomposite one, shears and inertia of rotation are taken into account. We use the high-order theory presented in [22], [23]. We introduce three projections of displacements. We denote the projections of the displacements of shell points on the generatrix of the cone by u_x; the projection of displacements on the circumferential coordinate, by u_φ; the projection on the normal to the median surface of the shell, by u_z. Following [22], [23], the projections of displacements can be represented as follows:

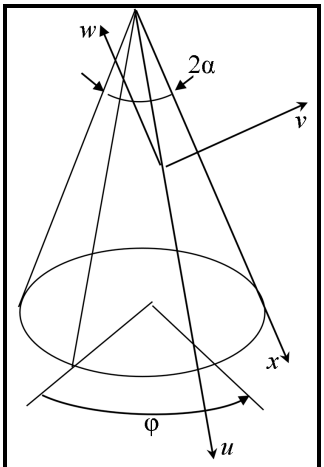

Fig. 2. A sketch of the conical shell

$$u_x = u(x,\varphi,t) + z\psi_x(x,\varphi,t) + z^2\theta_x + z^3\gamma_x, \; u_\varphi = \left(1+\frac{z}{R_\varphi}\right)v(x,\varphi,t) + z\psi_\varphi(x,\varphi,t) + z^2\theta_\varphi + z^3\gamma_\varphi, \; u_z = w(x,\varphi,t), \quad (1)$$

where u, v, w are the projections of the displacements of the points of the median surface onto the generatrix, circumferential coordinate, and normal to the median surface. The decomposition coefficients $\theta_x, \gamma_x, \theta_\varphi, \gamma_\varphi$ are unknown; they are derived from the boundary conditions

$$\tau_{xz}\big|_{z=\pm 0.5h} = \tau_{\varphi z}\big|_{z=\pm 0.5h} = 0, \quad (2)$$

where *h* is the thickness of the shell. The shear stresses on the upper and lower surfaces of the shell are zero. These boundary conditions can be rewritten with respect to the corresponding shear strains $\gamma_{xz}, \gamma_{\varphi z}$, which satisfy the relations

$$\gamma_{xz} = \frac{\partial u_x}{\partial z} + \frac{\partial u_z}{\partial x}, \quad \gamma_{\varphi z} = \frac{\partial u_\varphi}{\partial z} + \frac{1}{1+zR_\varphi^{-1}}\left(\frac{\partial u_z}{r\partial\varphi} - \frac{u_\varphi}{R_\varphi}\right). \quad (3)$$

We introduce expansion (1) into relation (3) and take into account the result in the boundary conditions (2). Then we derive the following relations for $\theta_x, \gamma_x, \theta_\varphi, \gamma_\varphi$

$$\theta_x = 0, \quad \gamma_x = -\frac{4}{3h^2}\left(\frac{\partial w}{\partial x} + \psi_x\right), \quad \theta_\varphi = \frac{1}{2R_\varphi r}\frac{\partial w}{\partial \varphi} + \frac{1}{2R_\varphi}\psi_\varphi, \quad \gamma_\varphi = -\frac{8R_\varphi^2 + h^2}{6R_\varphi^2 h^2}\psi_\varphi - \frac{\left(8R_\varphi^2 - h^2\right)}{6r\ h^2 R_\varphi^2}\frac{\partial w}{\partial \varphi} - \frac{v}{3R_\varphi^3}.$$

Further, the problem of non-stationary structural vibrations will be solved in displacements with respect to the five unknowns $u(x,\varphi,t), v(x,\varphi,t), w(x,\varphi,t), \psi_x(x,\varphi,t), \psi_\varphi(x,\varphi,t)$. To write the equations of motion of the structure, we use the assumed-modes method [24]. In order to use this method, it is necessary to obtain the expression for the potential and kinetic energy as a function of displacements. First of all, we derive the relations that connect strains and displacement components. For this, we use the relations presented in [23]. We write these relations for the conical shell. As a result, the elements of the strain tensor can be represented as follows:

$$\varepsilon_{xx} = \varepsilon_{x,0} + z\left(k_x^{(0)} + zk_x^{(1)} + z^2 k_x^{(2)}\right), \quad \varepsilon_{\varphi\varphi} = \varepsilon_{\varphi,0} + z\left(k_\varphi^{(0)} + zk_\varphi^{(1)} + z^2 k_\varphi^{(2)}\right),$$

$$\gamma_{x\varphi} = \gamma_{x\varphi,0} + z\left(k_{x\varphi}^{(0)} + zk_{x\varphi}^{(1)} + z^2 k_{x\varphi}^{(2)}\right), \quad \gamma_{xz} = \gamma_{xz,0} + z\left(k_{xz}^{(0)} + zk_{xz}^{(1)} + z^2 k_{xz}^{(2)}\right), \tag{4}$$

$$\gamma_{\varphi z} = \gamma_{\varphi z,0} + z\left(k_{\varphi z}^{(0)} + zk_{\varphi z}^{(1)} + z^2 k_{\varphi z}^{(2)}\right),$$

where $\varepsilon_{x,0}, \varepsilon_{\varphi,0}, \gamma_{x\varphi,0}, \gamma_{xz,0}, \gamma_{\varphi z,0}$, $k_x^{(0..2)}, k_\varphi^{(0..2)}, k_{x\varphi}^{(0..2)}, k_{xz}^{(0..2)}, k_{\varphi z}^{(0..2)}$ are differential expressions with respect to the unknowns $u(x,\varphi,t)$, $v(x,\varphi,t)$, $w(x,\varphi,t)$, $\psi_x(x,\varphi,t)$, $\psi_\varphi(x,\varphi,t)$.

We write the potential energy of the conical shell as follows [23], [25]:

$$\prod = 0{,}5\iiint_V \left\{Q_{11}(z)\varepsilon_{xx}^2 + 2Q_{12}(z)\varepsilon_{\varphi\varphi}\varepsilon_{xx} + Q_{22}(z)\varepsilon_{\varphi\varphi}^2 + G_{23}(z)\gamma_{\varphi z}^2 + G_{13}(z)\gamma_{xz}^2 + G_{21}(z)\gamma_{x\varphi}^2\right\}\left(1 + \frac{z}{R_\varphi}\right)dz r dx d\varphi, \tag{5}$$

where V is the volume occupied by the conical shell. We introduce expansions (4) into the potential energy (5) and expand in powers of z. Then the potential energy can be represented in the following form:

$$\prod = 0{,}5\iint_A r dx d\varphi \sum_{j=0}^{5} h_j, \tag{6}$$

where A is the region of the median surface of the conical shell; $h_0 = P_0^{(0)}$, $h_j = P_j^{(j)} + \frac{P_{j-1}^{(j)}}{R_\varphi}; j = 1,\ldots,5$, $P_{0..5}^{(j)}$ are the quadratic forms of the expressions $\varepsilon_{x,0}, \varepsilon_{\varphi,0}, \gamma_{x\varphi,0}, \gamma_{xz,0}, \gamma_{\varphi z,0}$, $k_x^{(0..2)}, k_\varphi^{(0..2)}, k_{x\varphi}^{(0..2)}, k_{xz}^{(0..2)}, k_{\varphi z}^{(0..2)}$.

We write the kinetic energy of the conical shell as follows [23], [25]:

$$T = 0{,}5\iiint_V \rho(z)\left(\dot{u}_x^2 + \dot{u}_\varphi^2 + \dot{u}_z^2\right)\left(1 + \frac{z}{R_\varphi}\right)dz r dx d\varphi, \tag{7}$$

where $\dot{u}_x = \frac{du_x}{dt}$.

We introduce expansion (1) into the kinetic energy (7). Then it takes the following form:

$$T = 0{,}5\iint_A r dx d\varphi \sum_{j=0}^{5} r_j P_j, \tag{8}$$

where $r_j = \int_{-0{,}5h}^{0{,}5h} z^j \rho(z) dz; j = 0,1,\ldots;$ $P_{0..5}$ are the quadratic forms of the velocities $\dot{u}$, $\dot{v}$, $\dot{w}$, $\dot{\psi}_x$, $\dot{\psi}_\varphi$ as well as expressions $\dot{\gamma}_x$, $\dot{\gamma}_\varphi$, $\dot{\theta}_\varphi$.

Consider the non-stationary dynamics of the structure due to the actuation of pyrodevices. Note that there can be any number of such devices. Further, we consider v of such devices. They are located on the upper section of the conical shell (Fig. 3). Their positions are determined by the circumferential coordinates of the cone $\varphi_j; j = 1,...,v$. The action of the pyrodevices is described by the shock loading, which is represented as the concentrated force

$$Q = \begin{cases} Q_0 \sin\left(\dfrac{\pi t}{T}\right), 0 \le t \le T \\ 0, \quad t > T \end{cases}, \tag{9}$$

where T is the action time of the shock load.

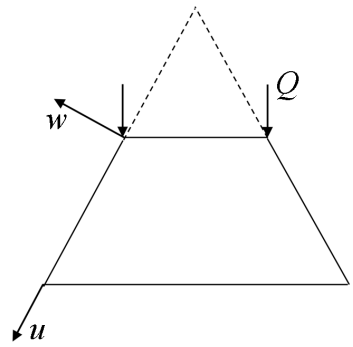

Fig. 3. The action of shock loads on the shell

The parameter Q_0 is determined by a given pulse value. The concentrated forces Q are directed perpendicular to the lower base of the cone. The virtual work from the action of all shock loads is derived as follows:

$$\delta A = -\int_0^{2\pi} F_w \delta w(L_1, \varphi, t) d\varphi + \int_0^{2\pi} F_u \delta u(L_1, \varphi, t) d\varphi,$$

where $F_w = \sin(\alpha)\sum_{j=1}^{v} Q_0 \sin\left(\dfrac{\pi t}{T}\right)\delta(\varphi - \varphi_j)$; $F_u = \cos(\alpha)\sum_{j=1}^{v} Q_0 \sin\left(\dfrac{\pi t}{T}\right)\delta(\varphi - \varphi_j)$; L_1 is the value of the longitudinal coordinate x in the upper section of the truncated cone. Finally, we write the virtual work expression in the form

$$\delta A = -\sin(\alpha) Q_0 \sin\left(\frac{\pi t}{T}\right)\sum_{j=1}^{v} \delta w(L_1, \varphi_j, t) + \cos(\alpha) Q_0 \sin\left(\frac{\pi t}{T}\right)\sum_{j=1}^{v} \delta u(L_1, \varphi_j, t). \tag{10}$$

Further, we will consider the conical shell clamped from below (Fig. 2). On the clamped side, the following boundary conditions are satisfied:

$$u\big|_{x=L_2} = v\big|_{x=L_2} = w\big|_{x=L_2} = \psi_x\big|_{x=L_2} = \psi_\varphi\big|_{x=L_2} = 0.$$

Analysis of Eigenfrequencies and Eigenvibrations

The non-stationary response of the conical shell is expanded in a series of its eigenvibrations. To analyze the eigenfrequencies and eigenvibrations of the conical shell, the Rayleigh-Ritz method [25, 26] is used. The main unknowns of the problem are the displacements and rotation angles of the normal. We represent the eigenvibrations of the conical shell in the following form:

$$\begin{bmatrix} u \\ v \\ w \\ \psi_x \\ \psi_y \end{bmatrix} = \begin{bmatrix} U_n(x)\cos(n\varphi) \\ V_n(x)\sin(n\varphi) \\ W_n(x)\cos(n\varphi) \\ X_n(x)\cos(n\varphi) \\ Y_n(x)\sin(n\varphi) \end{bmatrix} \cos(\omega t), \tag{11}$$

where ω is the eigenfrequency of the structure; n is the number of waves in the circumferential direction. The functions $U_n(x), V_n(x), , W_n(x), X_n(x), Y_n(x)$ are expanded in a series of trial functions as follows:

$$\begin{bmatrix} U_n(x) \\ V_n(x) \\ W_n(x) \\ X_n(x) \\ Y_n(x) \end{bmatrix} = \sum_{i=1}^{N} \begin{bmatrix} A_i \\ A_{N+i} \\ A_{2N+i} \\ A_{3N+i} \\ A_{4N+i} \end{bmatrix} \vartheta_i(x), \tag{12}$$

where $[A_1,\ldots,A_{5N}]$ are the unknown parameters that are calculated as a result of applying the Rayleigh-Ritz method.

To study cantilevered truncated cones as the trial functions $\vartheta_i(x)$, we choose: $\vartheta_i(x)=\sin\left[\dfrac{(2i-1)\pi(L_2-L_1-x)}{2(L_2-L_1)}\right]$. We substitute expansion (11) into the kinetic and potential energies (6, 7), which leads to the following expressions:

$$T=\omega^2\sin^2(\omega t)T,\quad \prod=\cos^2(\omega t)\prod. \tag{13}$$

We use the principle of least action, on the basis of which we can write [27]

$$\delta\int_0^{2\pi/\omega}(T-\prod)dt=0. \tag{14}$$

From expression (14), taking into account (12) and (13), we can find the eigenfrequencies and eigenvibrations of the shell.

Equations of Non-stationary Structural Responses

The eigenfrequencies ω_i and eigenvibrations $A^{(i)}$ are determined from the problem of eigenvalues. The found relations are introduced into (12). The result is a set of eigenvibrations in the form $U_n^{(i)}(x), V_n^{(i)}(x), W_n^{(i)}(x), X_n^{(i)}(x), Y_n^{(i)}(x)$.

We expand the non-stationary dynamics of the structure under the action of shock loading (9) in a series of eigenvibrations as follows:

$$u=\sum_{j=1}^{N_*}U_n^{(j)}(x)\,q_j(t)\cos(n_j\varphi),\quad v=\sum_{j=1}^{N_*}V_n^{(j)}(x)\,q_{N_*+j}(t)\sin(n_j\varphi),\quad w=\sum_{j=1}^{N_*}W_n^{(j)}(x)\,q_{2N_*+j}(t)\cos(n_j\varphi),$$

$$\psi_x=\sum_{j=1}^{N_*}X_n^{(j)}(x)\,q_{3N_*+j}(t)\cos(n_j\varphi),\quad \psi_y=\sum_{j=1}^{N_*}Y_n^{(j)}(x)\,q_{4N_*+j}(t)\sin(n_j\varphi), \tag{15}$$

where $(n_1,\ldots n_N)$ is the set of wave numbers in the circumferential direction, which is determined by analyzing the eigenfrequencies of the structure; $(q_1,\ldots q_{10N_*})$ is the vector of generalized coordinates that describes the non-stationary structural response.

We introduce expansions (15) into the structure's potential energy (6) and the kinetic energy (8). We make the necessary integration. Then, as a result, we get

$$\prod=0.5\sum_{i,k=1}^{10N_*}c_{ik}q_iq_k,\quad T=0.5\sum_{i,k=1}^{10N_*}m_{ik}\dot q_i\dot q_k.$$

From the virtual work expression (10), we find the generalized forces Q_i, corresponding to the generalized coordinate q_i in the form

$$Q_{2i}=Q_0\cos(\alpha)\sin\left(\frac{\pi t}{T}\right)U_n^{(i)}(L_1)\,C_i,\quad Q_{4N+2i}=-Q_0\sin(\alpha)\sin\left(\frac{\pi t}{T}\right)W_n^{(i)}(L_1)\,C_i,$$

$$C_i=\sum_{j=1}^{v}\cos(n_j\varphi_j),\quad i=1,\ldots,N_*.$$

Ordinary differential equations of non-stationary structural responses can be represented in the following matrix form:

$$\mathbf{M}\ddot{\mathbf{q}}+\mathbf{C}\mathbf{q}=\mathbf{Q}, \tag{16}$$

where $\mathbf{Q}=\{Q_1,\ldots,Q_{10N_*}\}$ is the vector of generalized forces.

To study the linear dynamical system (16), a numerical integration of these equations of motion is used.

Numerical Structural Dynamic Analysis

Consider the eigenfrequencies and eigenvibrations of the truncated conical shell, which is shown in Fig. 4. The geometry of the cone is described by the following parameters: L_1=0.225 m; L_2=0.5 m; h=5×10^{-3} m.

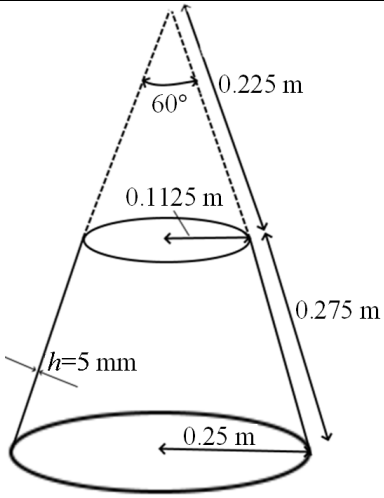

Fig. 4. A sketch of the truncated conical shell

The eigenfrequencies were calculated both by the Rayleigh-Ritz method and the finite element method, which is implemented in the ANSYS software suite. The calculation results of the eigenfrequencies of the truncated cone are presented in table 1. The first column of the table shows the calculation number; the second one, the eigenfrequency number. The third column shows the number of the circumferential waves that are observed during vibrations with the corresponding frequency. The fourth column shows the number of the trial functions that are used in expansions (15). The fifth column shows the number of the nodes in the longitudinal direction of the conical shell, which are observed during vibrations with the corresponding frequency. The sixth and seventh columns show the eigenfrequencies obtained by the Rayleigh-Ritz method and the finite element method. The eighth column shows the relative difference in the eigenfrequencies obtained by the two methods. From the first four rows of the table, it follows that seven trial functions in expansions (15) are enough to obtain eigenfrequencies with sufficient accuracy.

Table 1 presents the first twenty-sixth eigenfrequencies. It should be emphasized that for all eigenfrequencies, the results obtained by the Rayleigh-Ritz method and the finite element method (FEM) are close.

Study the non-stationary processes that occur in the conical shell (Fig. 3), with the parameters presented above, under the action of two shock loads Q (10), which have such circumferential coordinates: φ_1=0; φ_2=π. These shock loads are located on two opposite sides of the conical shell perpendicular to its base. The duration of this shock load T=5·10^{-4} secs and Q_0=3454 N. Constant reinforcement over the thickness of the UD nanocomposite was considered.

For FEM calculations, the commercial ANSYS software suite was used. The forms of shell displacements at times t=1.425·10^{-3} secs and t=1.085·10^{-3} secs are given in Fig. 5. As can be seen in the figure, in the non-stationary vibrations of the shell, there are several eigenvibrations.

Table 1. Eigenfrequencies of the cantilever truncated conical shell

Calculation number	Eigenfrequency number	Wave number	N	I_1	ω_i, Hz	FEM ω_i, Hz	δ
1	1	3	7	1	533.71	539.67	0.0110
2	2	4	7	1	554.68	562.28	0.0130
3	3	2	7	1	648.83	655.11	0.0095
4	4	5	7	1	679.46	691.51	0.0170
5	5	6	7	1	856.46	872.32	0.0180
6	6	1	7	1	953.70	958.00	0.0045
7	7	7	7	1	1046.63	1064.80	0.0170
8	8	4	7	2	1247.73	1217.40	0.0250
9	9	5	7	2	1284.93	1261.20	0.0180
10	10	8	7	1	1239.57	1263.30	0.0180
11	11	3	7	2	1298.05	1271.70	0.0200
12	12	6	7	2	1412.07	1406.00	0.0040
13	13	2	7	2	1456.26	1442.50	0.0090
14	14	9	7	1	1442.42	1474.90	0.0200
15	15	7	7	2	1631.96	1651.90	0.0120
16	1	10	7	1	1660.02	1702.50	0.0250
17	17	1	7	2	1762.81	1768.00	0.0030
18	18	11	7	1	1893.00	1949.70	0.0280
19	19	8	7	2	1921.09	1962.80	0.0210
20	20	12	7	1	2140.20	2208.10	0.0300
21	21	9	7	2	2237.00	2293.80	0.0240
22	22	4	7	3	2464.41	2438.70	0.0100
23	23	5	7	3	2466.51	2443.50	0.0090
24	24	13	7	1	2400.92	2480.20	0.0300
25	25	3	7	3	2510.20	2485.20	0.0100
26	26	6	7	3	2514.33	2496.60	0.0070

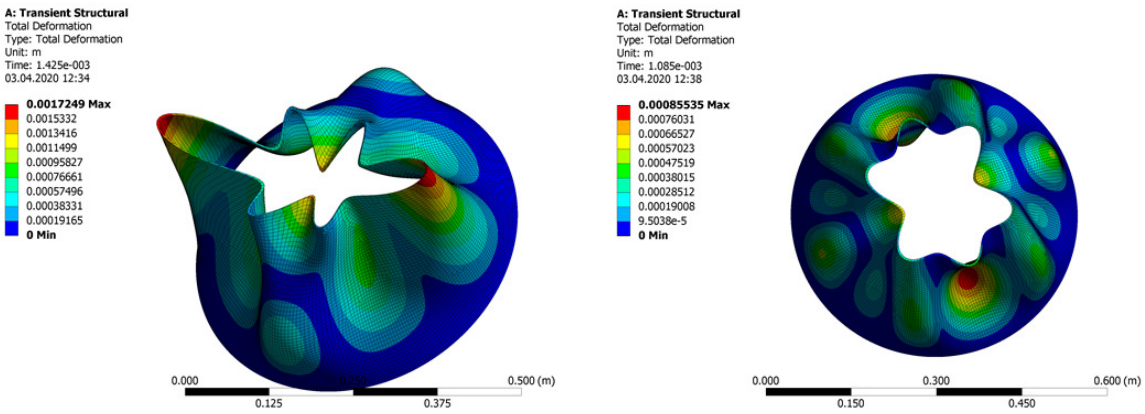

a b

Fig. 5. The form of displacements of the conical shell at times: a – t=1.425·10^{-3} secs; b – t=1.085·10^{-3} secs

Consider the case of two pyrodevices located at diametrically opposite points of the median surface of the truncated cone. Then φ_1=0; φ_2=π. For the numerical modeling of non-stationary dynamic processes, the above-derived linear dynamic model was used. The dynamical system (16) was numerically integrated using the Runge-Kutta method with a variable pitch.

Convergence of non-stationary dynamic processes in the conical structure was studied, which is described by the dynamic system (16). In this case, the calculations took into account a different number of terms in expansion (15). Three dynamic models were built. The first model has 10 degrees of freedom in expansion (15). In this case, the solutions are expanded in a series of eigenvibrations 5 and 8 (Table 1). The second dynamic model has 30 degrees of freedom. In this case, solution (15) is expanded in a series of six eigenvibrations with numbers 5; 8; 10; 12; 13; 16 (Table 1). The third dynamic model has 60 degrees of freedom. In this case, solution (15) is expanded in a series of 12 eigenvibrations with numbers 2; 3; 5; 8; 10; 12; 13; 16; 19; 20; 22; 26 (Table 1). The results of the analysis of the dynamic processes described by these three models are presented in Fig. 6.

Fig. 6 shows the results of the numerical integration of the dynamical system with a different number of degrees of freedom (the solid bold line, with 10 degrees of freedom; the solid thin line, with 30 degrees of freedom; the dashed line, with 60 degrees

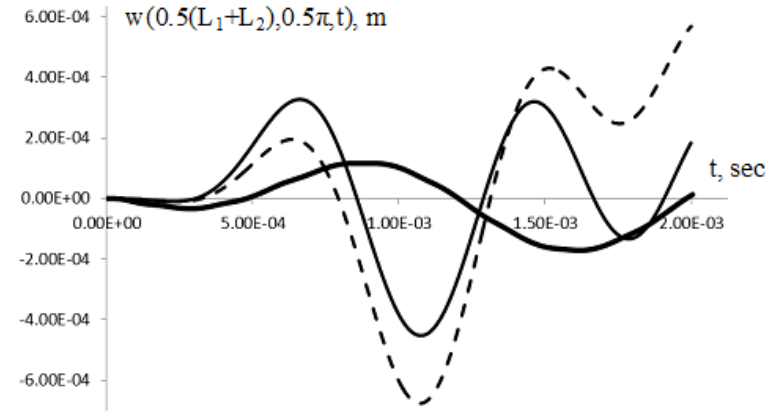

Fig. 6. Transient convergence analysis

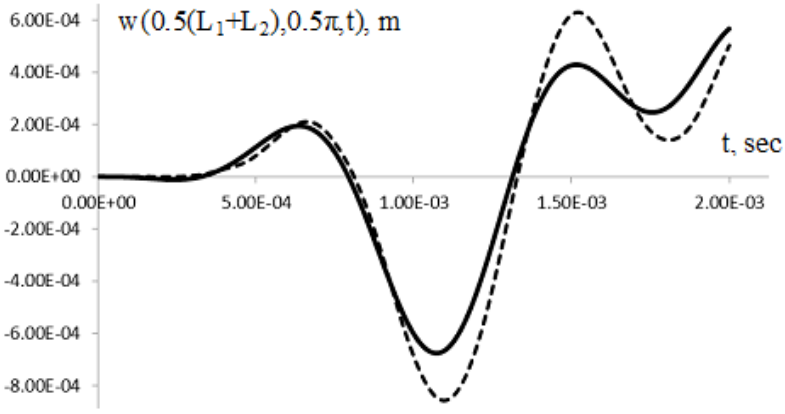

Fig. 7. Comparison of the obtained results with the simulation results in the ANSYS software suite

of freedom). So, the three non-stationary dynamic processes are significantly different. Compare the obtained results with the simulation results in the ANSYS software suite. The results of this comparison are presented in Fig. 7.

In this figure, the solid line shows the results of the numerical integration of the dynamical system (16) with 60 degrees of freedom, and the dashed one shows the results obtained in the commercial ANSYS software suite. The *y*-axis in this figure shows

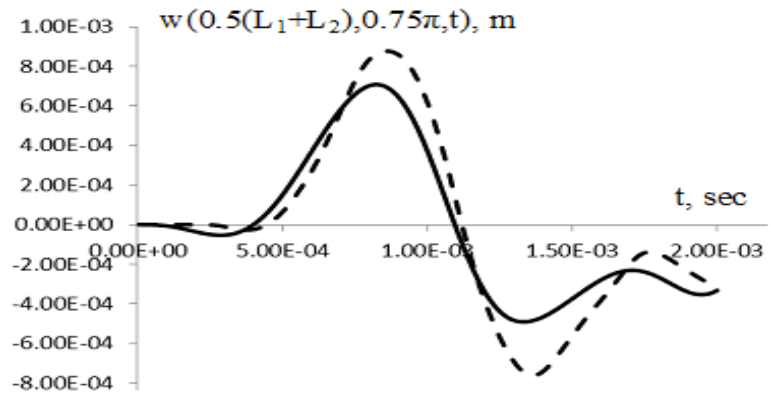

Fig. 8. Comparison of the obtained results with the simulation results in the ANSYS software suite

the transversal displacements w at the point $x=0.5(L_1+L_2)$; $\varphi=0.5\pi$. The dynamic process obtained in the ANSYS software suite and the dynamic process obtained according to model 3 are close. Therefore, we assume that the third model adequately describes the dynamic process.

The transverse displacements w at another point, $x=0.5(L_1+L_2)$; $\varphi=0.75\pi$, obtained on the basis of model 3, were compared with the simulation results in the ANSYS software suite. The results of this comparison are shown in Fig. 8, where the solid line shows the results of integration according to model 3, and the dashed one shows the results of calculation in the ANSYS software suite. So, the results obtained by these two methods are close.

Conclusions

A method for the analysis of the transient processes arising in a carbon nanotube-reinforced composite truncated conical shell under the influence of shock loading is proposed. The results are compared with the finite element simulation results. The method allows us to evaluate the influence of shock loading on the shell with the required accuracy.

References

1. Seidel, G. D. & Lagoudas, D. C. (2006). Micromechanical analysis of the effective elastic properties of carbon nanotube reinforced composites. *Mechanics of Materials*, vol. 38, iss. 8–10, pp. 884–907. https://doi.org/10.1016/j.mechmat.2005.06.029.
2. Liu, Y. J. & Chen, X. L. (2003). Evaluations of the effective material properties of carbon nanotube-based composites using a nanoscale representative volume element. *Mechanics of Materials*, vol. 35, iss. 1–2, pp. 69–81. https://doi.org/10.1016/S0167-6636(02)00200-4.
3. Odegard, G. M., Gates, T. S., Wise, K. E., Park, C., & Siochi, E. J. (2003). Constitutive modeling of nanotube–reinforced polymer composites. *Composites Science and Technology,* vol. 63, iss. 11, pp. 1671–1687. https://doi.org/10.1016/S0266-3538(03)00063-0.
4. Allaoui, A., Bai, S., Cheng, H. M., & Bai, J. B. (2002). Mechanical and electrical properties of a MWNT/epoxy composite. *Composites Science and Technology*, vol. 62, iss. 15, pp. 1993–1998. https://doi.org/10.1016/S0266-3538(02)00129-X.
5. Kanagaraj, S., Varanda, F. R., Zhil'tsova, T. V., Oliveira, M. S. A., & Simoes, J. A. O. (2007). Mechanical properties of high density polyethylene/carbon nanotube composites. *Composites Science and Technology*, vol. 67, iss. 15–16, pp. 3071–3077. https://doi.org/10.1016/j.compscitech.2007.04.024.
6. Nejati, M., Asanjarani, A., Dimitri, R., Tornabene, F. (2017). Static and free vibration analysis of functionally graded conical shells reinforced by carbon nanotubes. *International Journal of Mechanical Sciences*, vol. 130, pp. 383–398. https://doi.org/10.1016/j.ijmecsci.2017.06.024.
7. Hu, H., Onyebueke, L., & Abatan, A. (2010). Characterizing and modeling mechanical properties of nanocomposites. Review and evaluation. *Journal of Minerals & Materials Characterization & Engineering*, vol. 9, no. 4, pp. 275–319. https://doi.org/10.4236/jmmce.2010.94022.
8. Mehrabadi, S. J. & Aragh, B. S. (2014). Stress analysis of functionally graded open cylindrical shell reinforced by agglomerated carbon nanotubes. *Thin-Walled Structures*, vol. 80, pp. 130–141. https://doi.org/10.1016/j.tws.2014.02.016.

9. Zhang, L. W., Lei, Z. X., Liew, K. M., & Yu, J. L. (2014). Static and dynamic of carbon nanotube reinforced functionally graded cylindrical panels. *Composite Structures*, vol. 111, pp. 205–212. https://doi.org/10.1016/j.compstruct.2013.12.035.
10. Song, Z. G., Zhang, L. W., & Liew, K. M. (2016). Vibration analysis of CNT-reinforced functionally graded composite cylindrical shells in thermal environments. *International Journal of Mechanical Sciences*, vol. 115–116, pp. 339–347. https://doi.org/10.1016/j.ijmecsci.2016.06.020.
11. Sobhaniaragh, B., Batra, R. C., Mansur, W. J., & Peters, F. C. (2017). Thermal response of ceramic matrix nanocomposite cylindrical shells using Eshelby-Mori-Tanaka homogenization scheme. *Composites Part B: Engineering*, vol. 118, pp. 41–53. https://doi.org/10.1016/j.compositesb.2017.02.032.
12. Yaser, K., Rossana, D., & Francesco, T. (2018). Free vibration of FG-CNT reinforced composite skew cylindrical shells using the Chebyshev-Ritz formulation. *Composites Part B: Engineering*, vol. 147, pp. 169–177. https://doi.org/10.1016/j.compositesb.2018.04.028.
13. Lei, Z. X., Liew, K. M., & Yu, J. L. (2013). Free vibration analysis of functionally graded carbon nanotube-reinforced composite plates using the element-free kp-Ritz method in thermal environment. *Composite Structures*, vol. 106, pp. 128–138. https://doi.org/10.1016/j.compstruct.2013.06.003.
14. Lei, Z. X., Zhang, L. W., & Liew, K. M. (2015). Elastodynamic analysis of carbon nanotube-reinforced functionally graded plates. *International Journal of Mechanical Sciences*, vol. 99, pp. 208–217. https://doi.org/10.1016/j.ijmecsci.2015.05.014.
15. García-Macías, E., Rodríguez-Tembleque, L., & Sáez, A. (2018). Bending and free vibration analysis of functionally graded graphene vs. carbon nanotube reinforced composite plates. *Composite Structures*, vol. 186, pp. 123–138. https://doi.org/10.1016/j.compstruct.2017.11.076.
16. Wang, Q., Cui, X., Qin, B., & Liang, Q. (2017). Vibration analysis of the functionally graded carbon nanotube reinforced composite shallow shells with arbitrary boundary conditions. *Composite Structures*, vol. 182, pp. 364–379. https://doi.org/10.1016/j.compstruct.2017.09.043.
17. Wang, A., Chen, H., Hao, Y., & Zhang, Y. (2018). Vibration and bending behavior of functionally graded nanocomposite doubly-curved shallow shells reinforced by graphene nanoplatelets. *Results in Physics*, vol. 9, pp. 550–559. https://doi.org/10.1016/j.rinp.2018.02.062.
18. Moradi-Dastjerdi, R., Foroutan, M., & Pourasghar, A. (2013). Dynamic analysis of functionally graded nanocomposite cylinders reinforced by carbon nanotube by a mesh-free method. *Materials and Design*, vol. 44, pp. 256–266. https://doi.org/10.1016/j.matdes.2012.07.069.
19. Shen, H.-S. (2009). Nonlinear bending of functionally graded carbon nanotube-reinforced composite plates in thermal environments. *Composite Structures*, vol. 91, iss. 1, pp. 9–19. https://doi.org/10.1016/j.compstruct.2009.04.026.
20. Wang, Q., Qin, B., Shi, D., & Liang, Q. (2017). A semi-analytical method for vibration analysis of functionally graded carbon nanotube reinforced composite doubly-curved panels and shells of revolution. *Composite Structures*, vol. 174, pp. 87–109. https://doi.org/10.1016/j.compstruct.2017.04.038.
21. Reddy, J. N. (1984). A simple higher-order theory for laminated composite plates. *ASME Journal of Applied Mechanics*, vol. 51, iss. 4, pp. 745–752. https://doi.org/10.1115/1.3167719.
22. Reddy, J. N. (1984). A refined nonlinear theory of plates with transverse shear deformation. *International Journal of Solids and Structures*, vol. 20, iss. 9–10, pp. 881–896. https://doi.org/10.1016/0020-7683(84)90056-8.
23. Amabili, M. (2010). A new non-linear higher-order shear deformation theory for large-amplitude vibrations of laminated doubly curved shells. *International Journal of Non-Linear Mechanics*, vol. 45, iss. 4, pp. 409–418. https://doi.org/10.1016/j.ijnonlinmec.2009.12.013.
24. Meirovitch, L. (1986). Elements of vibration analysis. New York: McGraw-Hill Publishing Company, 560 p.
25. Avramov, K., Chernobryvko, M., Uspensky, B., Seitkazenova, K., & Myrzaliyev, D. (2019). Self-sustained vibrations of functionally graded carbon nanotubes reinforced composite cylindrical shell in supersonic flow. *Nonlinear Dynamics*, vol. 98, no. 3, pp. 1853–1876. https://doi.org/10.1007/s11071-019-05292-z.
26. Chernobryvko, M. V., Avramov, K. V., Romanenko, V. N., Batutina, T. J., & Tonkonogenko, A. M. (2014). Free linear vibrations of thin axisymmetric parabolic shells. *Meccanica*, vol. 49, no. 8, pp. 2839–2845. https://doi.org/10.1007/s11012-014-0027-6.
27. Gantmakher, F. R. (1966). *Lektsii po analiticheskoy mekhanike* [Lectures on analytical mechanics]. Moscow: Nauka, 300 p. (in Russian).

Received 30 April 2020

Нестаціонарний відгук конічної композитної оболонки, посиленої вуглецевими нанотрубками

К. В. Аврамов, Б. В. Успенський, Н. Г. Сахно, І. В. Біблік

Інститут проблем машинобудування ім. А. М. Підгорного НАН України,
61046, Україна, м. Харків, вул. Пожарського, 2/10

Стаття присвячена розробці методу аналізу нестаціонарного деформування нанокомпозитної оболонки під впливом імпульсного навантаження. Розвиток інноваційних виробничих технологій привів до виникнення нових матеріалів, які мають високий потенціал для використання в аерокосмічній промисловості. До них, зокрема, належать матеріали, які армовано вуглецевими нанотрубками (ВНТ) – так звані нанокомпозити. Ці матеріали демонструють високу міцність та жорсткість в поєднанні з малою масою, що є надзвичайно актуальним під час проєктування елементів ракетних та авіаційних конструкцій: обтічників, паливних баків, двигунів. Водночас, поведінка елементів конструкцій за характерних впливів зовнішнього середовища потребує додаткового дослідження внаслідок анізотропних та функціонально-градієнтних властивостей матеріалу. Визначення механічних властивостей нанокомпозитного матеріалу викликає деяку складність внаслідок його нанокомпозитної природи. Існують різні підходи до розв'язання цієї проблеми. Модифіковане правило змішування є найпростішим і при цьому таким, що добре себе зарекомендувало. Його використано в роботі. Отримано рівняння руху конічної оболонки під впливом ударного навантаження. Для виводу рівнянь руху оболонки використано теорію високого порядку, яка враховує зсуви та інерцію обертання. Для аналізу нестаціонарної динаміки оболонки проведено аналіз її вільних коливань. Результати аналізу мають високу точність у порівнянні зі скінченно-елементним розрахунком, який проведено в програмному комплексі ANSYS. Запропоновано метод аналізу динамічного відгуку оболонки під впливом ударного навантаження, який базується на аналізі власних форм коливань конструкції. Отримано часові залежності деформацій адаптера для випадків спрацювання двох та чотирьох піропристроїв. Результати аналізу нестаціонарної динаміки адаптера було порівняно з результатами скінченно-елементного аналізу.

***Ключові слова**: конічна оболонка, імпульсне навантаження, нестаціонарний процес, нанокомпозитний матеріал.*

Література

1. Seidel G. D., Lagoudas D. C. Micromechanical analysis of the effective elastic properties of carbon nanotube reinforced composites. *Mechanics of Materials*. 2006. Vol. 38. Iss. 8–10. P. 884–907. https://doi.org/10.1016/j.mechmat.2005.06.029.
2. Liu Y. J., Chen X. L. Evaluations of the effective material properties of carbon nanotube-based composites using a nanoscale representative volume element. *Mechanics of Materials.* 2003. Vol. 35. Iss. 1–2. P. 69–81. https://doi.org/10.1016/S0167-6636(02)00200-4.
3. Odegard G. M., Gates T. S., Wise K. E., Park C., Siochi E. J. Constitutive modeling of nanotube–reinforced polymer composites. *Composites Sci. and Technology.* 2003. Vol. 63. Iss. 11. P. 1671–1687. https://doi.org/10.1016/S0266-3538(03)00063-0.
4. Allaoui A., Bai S., Cheng H. M., Bai J. B. Mechanical and electrical properties of a MWNT/epoxy composite. *Composites Sci. and Technology*. 2002. Vol. 62. Iss. 15. P. 1993–1998. https://doi.org/10.1016/S0266-3538(02)00129-X.
5. Kanagaraj S., Varanda F. R., Zhil'tsova T. V., Oliveira M. S. A., Simoes J. A. O. Mechanical properties of high density polyethylene/carbon nanotube composites. *Composites Sci. and Technology.* 2007. Vol. 67. Iss. 15–16. P. 3071–3077. https://doi.org/10.1016/j.compscitech.2007.04.024.
6. Nejati M., Asanjarani A., Dimitri R., Tornabene F. Static and free vibration analysis of functionally graded conical shells reinforced by carbon nanotubes. *Intern. J. Mech. Sci*. 2017. Vol. 130. P. 383–398. https://doi.org/10.1016/j.ijmecsci.2017.06.024.
7. Hu H., Onyebueke L., Abatan A. Characterizing and modeling mechanical properties of nanocomposites. Review and evaluation. *J. Minerals & Materials Characterization & Eng*. 2010. Vol. 9. No. 4. P. 275–319. https://doi.org/10.4236/jmmce.2010.94022.
8. Mehrabadi S. J., Aragh B. S. Stress analysis of functionally graded open cylindrical shell reinforced by agglomerated carbon nanotubes. *Thin-Walled Structures.* 2014. Vol. 80. P. 130–141. https://doi.org/10.1016/j.tws.2014.02.016.
9. Zhang L. W., Lei Z. X., Liew K. M., Yu J. L. Static and dynamic of carbon nanotube reinforced functionally graded cylindrical panels. *Composite Structures*. 2014. Vol. 111. P. 205–212. https://doi.org/10.1016/j.compstruct.2013.12.035.

10. Song Z. G., Zhang L. W., Liew K. M. Vibration analysis of CNT-reinforced functionally graded composite cylindrical shells in thermal environments. *Intern. J. Mech. Sci*. 2016. Vol. 115–116. P. 339–347. https://doi.org/10.1016/j.ijmecsci.2016.06.020.
11. Sobhaniaragh B., Batra R. C., Mansur W. J., Peters F. C. Thermal response of ceramic matrix nanocomposite cylindrical shells using Eshelby-Mori-Tanaka homogenization scheme. *Composites Part B: Engineering*. 2017. Vol. 118. P. 41–53. https://doi.org/10.1016/j.compositesb.2017.02.032.
12. Yaser K., Rossana D., Francesco T. Free vibration of FG-CNT reinforced composite skew cylindrical shells using the Chebyshev-Ritz formulation. *Composites Part B: Engineering*. 2018. Vol. 147. P. 169–177. https://doi.org/10.1016/j.compositesb.2018.04.028.
13. Lei Z. X., Liew K. M., Yu J. L. Free vibration analysis of functionally graded carbon nanotube-reinforced composite plates using the element-free kp-Ritz method in thermal environment. *Composite Structures.* 2013. Vol. 106. P. 128–138. https://doi.org/10.1016/j.compstruct.2013.06.003.
14. Lei Z. X., Zhang L. W., Liew K. M. Elastodynamic analysis of carbon nanotube-reinforced functionally graded plates. *Intern. J. Mech. Sci*. 2015. Vol. 99. P. 208–217. https://doi.org/10.1016/j.ijmecsci.2015.05.014.
15. García-Macías E., Rodríguez-Tembleque L., Sáez A. Bending and free vibration analysis of functionally graded graphene vs. carbon nanotube reinforced composite plates. *Composite Structures*. 2018. Vol. 186. P. 123–138. https://doi.org/10.1016/j.compstruct.2017.11.076.
16. Wang Q., Cui X., Qin B., Liang Q. Vibration analysis of the functionally graded carbon nanotube reinforced composite shallow shells with arbitrary boundary conditions. *Composite Structures*. 2017. Vol. 182. P. 364–379. https://doi.org/10.1016/j.compstruct.2017.09.043.
17. Wang A., Chen H., Hao Y., Zhang Y. Vibration and bending behavior of functionally graded nanocomposite doubly-curved shallow shells reinforced by graphene nanoplatelets. *Results in Physics*. 2018. Vol. 9. P. 550–559. https://doi.org/10.1016/j.rinp.2018.02.062.
18. Moradi-Dastjerdi R., Foroutan M., Pourasghar A. Dynamic analysis of functionally graded nanocomposite cylinders reinforced by carbon nanotube by a mesh-free method. *Materials and Design*. 2013. Vol. 44. P. 256–266. https://doi.org/10.1016/j.matdes.2012.07.069.
19. Shen H.-S. Nonlinear bending of functionally graded carbon nanotube-reinforced composite plates in thermal environments. *Composite Structures*. 2009. Vol. 91. Iss. 1. P. 9–19. https://doi.org/10.1016/j.compstruct.2009.04.026.
20. Wang Q., Qin B., Shi D., Liang Q. A semi-analytical method for vibration analysis of functionally graded carbon nanotube reinforced composite doubly-curved panels and shells of revolution. *Composite Structures*. 2017. Vol. 174. P. 87–109. https://doi.org/10.1016/j.compstruct.2017.04.038.
21. Reddy J. N. A simple higher-order theory for laminated composite plates. *ASME J. Appl. Mech*. 1984. Vol. 51. Iss. 4. P. 745–752. https://doi.org/10.1115/1.3167719.
22. Reddy J. N. A refined nonlinear theory of plates with transverse shear deformation. *Int. J. Solids and Structures*. 1984. Vol. 20. Iss. 9–10. P. 881–896. https://doi.org/10.1016/0020-7683(84)90056-8.
23. Amabili M. A new non-linear higher-order shear deformation theory for large-amplitude vibrations of laminated doubly curved shells. *Int. J. Non-Lin. Mech*. 2010. Vol. 45. Iss. 4. P. 409–418. https://doi.org/10.1016/j.ijnonlinmec.2009.12.013.
24. Meirovitch L. Elements of vibration analysis. New York: McGraw-Hill Publishing Company, 1986. 560 p.
25. Avramov K., Chernobryvko M., Uspensky B., Seitkazenova K., Myrzaliyev D. Self-sustained vibrations of functionally graded carbon nanotubes reinforced composite cylindrical shell in supersonic flow. *Nonlinear Dynamics*. 2019. Vol. 98. No. 3. P. 1853–1876. https://doi.org/10.1007/s11071-019-05292-z.
26. Chernobryvko M. V., Avramov K. V., Romanenko V. N., Batutina T. J., Tonkonogenko A. M. Free linear vibrations of thin axisymmetric parabolic shells. *Meccanica*. 2014. Vol. 49. No. 8. P. 2839–2845. https://doi.org/10.1007/s11012-014-0027-6.
27. Гантмахер Ф. Р. Лекции по аналитической механике. М.: Наука, 1966. 300 с.